Numerical simulation of the effect of recombination centres and traps created by electron irradiation on the performance degradation of GaAs solar cells

# Numerical simulation of the effect of recombination centres and traps created by electron irradiation on the performance degradation of GaAs solar cells

## A F Meftah[1,3], N Sengouga[1], A Belghachi[2] and A M Meftah[1]

[1] Laboratory of Metallic and Semiconducting Materials, Faculty of Science and Engineering, Mohamed Kheider University, BP 145, 07000 Biskra, Algeria
[2] Laboratory of Semiconductor Devices Physics, Physics Department, University of Béchar, PO Box 417, Béchar 08000, Algeria

E-mail: af_mef@yahoo.fr

## Abstract

In this paper, we report a detailed numerical study of the electron irradiation effect on the photoelectrical parameters of a GaAs based $p^+$–$n$–$n^+$ solar cell which operates under an AM0 solar spectrum. As a consequence of irradiation different types of defects are created in the semiconductor lattice. These defects introduce energy levels in the gap of the material. The majority of studies dealing with irradiation-induced degradation in solar cells relate it mainly to recombination centres, which are deep levels lying near the mid gap. In the present study, numerical simulation is used to demonstrate that the irradiation-induced degradation is not solely due to recombination centres. Other less deep levels, or traps, play a major role in this degradation. When only recombination centres are taken into account, the short circuit current density ($J_{sc}$) is hardly affected while the other cell output parameters such as the open circuit voltage ($V_{oc}$), the conversion efficiency ($\eta$) and the fill factor (FF) are strongly deteriorated. However, if less deep levels or traps are taken into account together with recombination centres, $J_{sc}$ becomes sensitive to electron irradiation and the other output parameter deteriorations become less sensitive.

## 1. Introduction

Photovoltaic based power sources for satellites require radiation resistant and high efficiency solar cells. Si, GaAs, InP and InGaP are exclusive materials that can meet both requirements because of their mature technology which can produce high quality materials as well as good doping control, see for example [1–4]. While Si offers the obvious advantage of more mature and relatively cheap technology, compound semiconductors have higher conversion efficiency and radiation resistance due to their higher absorption coefficient and direct larger energy band gap.

Among compound semiconductor materials, GaAs is commonly preferred for space applications because of its advanced technology [1]. When exposed to cosmic particle irradiations such as electrons and protons, GaAs solar cells undergo significant deterioration in their performance. This constitutes a serious problem for the power supplies of satellites operating in orbits. The mechanism of irradiation-induced degradation has been widely studied [2–8]. Electron irradiation, for example, introduces simple intrinsic defects, i.e. vacancies and interstitials that given rise to energy levels (recombination centres and traps) in the GaAs energy gap [4, 5]. Recombination centres have comparable capture cross sections for electrons and holes and energy levels near mid gap while traps have different capture cross sections for electrons and holes and energy levels that can be anywhere in the band gap. Recombination centres can significantly alter the free carrier lifetime while traps can affect the effective

---

[3] Author to whom any correspondence should be addressed.

doping density. It is believed that only deep levels are responsible for the photoelectrical performance degradation of the solar cell [4] by a decrease in the free carrier lifetime and hence in their diffusion length. Therefore recombination centres, instead of traps, are assumed to be responsible for this degradation since they are the most effective in the capture mechanism. This might be true if all energy levels have comparable capture cross sections and introduction rates so that they can be represented by a single level which has comparable capture cross sections for electrons and holes. This simplifies the development of an analytical relation between the solar cell parameter degradation and the recombination centre parameters [4, 7].

In practice, observed defects have a wide range of introduction rates and capture cross sections [5]. Moreover only capture cross section for the corresponding free carrier type can be calculated even by the most powerful technique, namely deep level transient spectroscopy [5]. It is, therefore, very difficult if not impossible to distinguish between recombination centres and traps. It is also difficult to relate the solar cell degradation to the parameters of the different defects by a simple analytical relation. Therefore the use of the simplified analytical procedure can lead to large errors in estimating recombination centre parameters. Extensive experimental and analytical work is therefore required to fully characterize the degradation of the solar cell performance. The experimental characterization turns out to be time consuming and can be very expensive.

Numerical simulation is a powerful tool which helps in understanding experimental observation and to relate irradiation-induced solar cell degradation to defects. Many parameters can be varied to model the observed phenomenon. It can also offer a physical explanation of the observed phenomenon since internal parameters such as the recombination rate and the free carrier densities can be calculated. In addition to all these advantages, numerical simulation can be used as a tool to predict output parameter degradation before any exposure to irradiation. It can also be used to estimate the lifetime of the solar cell.

In this paper we show by numerical simulation using the full Shockley–Read–Hall (SRH) statistics [9, 10] that recombination centres (deep levels) alone induce a strong unreasonable deterioration of $V_{oc}$, FF $\eta$ of the cell, while $J_{sc}$ is hardly affected. However, if other less deep levels are taken into account together with the deep ones, a reasonable degradation magnitude is observed for $V_{oc}$, FF $\eta$ while $J_{sc}$ becomes more sensitive to the electron irradiation.

## 2. Numerical modelling

The simulation program that we developed is based on the Kurata method [11], which is detailed in the appendix, and provides a one-dimensional numerical solution of the carrier transport problem in a GaAs $p^+$–n–$n^+$ solar cell subject to surface recombination velocity boundary conditions. A stationary simultaneous solution of Poisson's equation and hole and electron continuity equations, approximated by a

finite difference, is obtained. These equations are:

$$\frac{1}{q}\frac{\mathrm{d}J_\mathrm{n}}{\mathrm{d}x} + G(x) - \sum_j U_j(x) = 0 \tag{1a}$$

$$\frac{1}{q}\frac{\mathrm{d}J_\mathrm{p}}{\mathrm{d}x} - G(x) + \sum_j U_j(x) = 0 \tag{1b}$$

$$\frac{\mathrm{d}^2\Psi}{\mathrm{d}x^2} = -\frac{\rho(x)}{\varepsilon_0\varepsilon_\mathrm{r}} \tag{2}$$

where $J_\mathrm{n}$ and $J_\mathrm{p}$ are the electron and hole conduction current densities given by:

$$J_\mathrm{n} = -q\mu_\mathrm{n}n\frac{\mathrm{d}\psi}{\mathrm{d}x} + k_\mathrm{B}T\mu_\mathrm{n}\frac{\mathrm{d}n}{\mathrm{d}x} \tag{3a}$$

and

$$J_\mathrm{p} = -q\mu_\mathrm{p}p\frac{\mathrm{d}\psi}{\mathrm{d}x} - k_\mathrm{B}T\mu_\mathrm{p}\frac{\mathrm{d}p}{\mathrm{d}x} \tag{3b}$$

which obey the surface recombination velocity boundary conditions:

$$J_\mathrm{n}(0) = qS_\mathrm{n}(n(0) - n_\mathrm{eq}) \tag{4a}$$

$$J_\mathrm{p}(0) = qS_\mathrm{p}(p(0) - p_\mathrm{eq}) \tag{4b}$$

$$J_\mathrm{n}(d) = qS_\mathrm{n}(n(d) - n_\mathrm{eq}) \tag{4c}$$

$$J_\mathrm{p}(d) = qS_\mathrm{p}(p(d) - p_\mathrm{eq}) \tag{4d}$$

$n_\mathrm{eq}$ and $p_\mathrm{eq}$ are the equilibrium electron and hole densities respectively and $d$ is the sample thickness.

$G$ is the generation rate, $\mu_\mathrm{n}$ and $\mu_\mathrm{p}$ are the free electron and hole mobilities (8500 and 400 cm$^2$ V$^{-1}$ s$^{-1}$ respectively which are fairly acceptable values for low fields and doping densities [12]), $T$ is the absolute temperature (300 K), $\varepsilon_0 = 8.85 \times 10^{-14}$ F cm$^{-1}$ is the permittivity of the free space and $\varepsilon$ is the dielectric constant (12.9), $k_\mathrm{B}$ is the Boltzmann constant, $S_\mathrm{n} = S_\mathrm{p} = 10^8$ cm s$^{-1}$ are the assumed electron and hole recombination velocities at the structure boundaries, $\rho(x)$ is the space charge density and $U_j(x)$ is the non-radiative recombination rate of the $j$th defect given by SRH (Shockley–Read–Hall) statistics [9, 10]:

$$U_j = \frac{(n \cdot p - n_\mathrm{i}^2)}{\tau_{\mathrm{p}j}(n + n_{1j}) + \tau_{\mathrm{n}j}(p + p_{1j})} \tag{5}$$

where $\tau_{\mathrm{n}j}$ and $\tau_{\mathrm{p}j}$ are the minority carrier lifetimes which are related to the defect level by $\tau_{\mathrm{n}j} = 1/\sigma_{\mathrm{n}j}v_\mathrm{th}N_j$, $\tau_{\mathrm{p}j} = 1/\sigma_{\mathrm{p}j}v_\mathrm{th}N_j$, where $\sigma_{\mathrm{n}j}$ and $\sigma_{\mathrm{p}j}$ are the capture cross sections for electrons and holes, respectively, $v_\mathrm{th} \sim 10^7$ cm s$^{-1}$ is the thermal velocity, $N_j$ is the defect density $n_\mathrm{i}$ is the intrinsic density of GaAs which is $\approx 2.1 \times 10^6$ cm$^{-3}$ and $n_{1j}$ and $p_{1j}$ are the electron and hole densities when their quasi-Fermi levels coincide with the defect level. Relation (5) allows introducing many defect levels and studying their effect in detail since their energy position and capture cross section are taken into account. However, the simplified formula ($U_{\mathrm{n(p)}} = \Delta n(p)/\tau_{\mathrm{n(p)}}$; $\tau^{-1} = \tau_0^{-1} + \sigma v_\mathrm{th}N_\mathrm{r}$) commonly used [5, 6, 13] takes into account only one defect (the most dominant recombination centre which is supposed to be exactly at mid gap) so that the fitting of experimental data to the
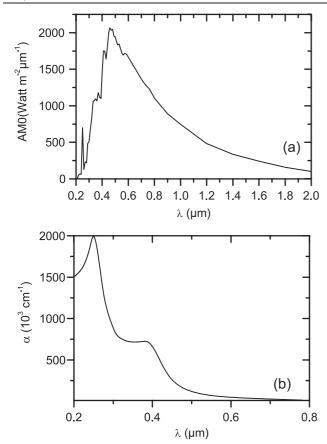
**Figure 1.** The AM0 solar spectrum (a) [15] and the absorption coefficient for GaAs (b) [16].

**Table 1.** Parameters of electron ($E_i$) and hole traps ($H_i$) induced in GaAs by electron irradiation from [4, 5]; $k$ is the introduction rate of defects, $E_t$ the defect level position, $\sigma_n$ and $\sigma_p$ the capture cross sections of electrons and holes, respectively.

| Defects | $k$ (cm$^{-1}$) (Introduction rate) | $E_C$–$E_T$ (eV) | $\sigma_n$ (cm$^2$) |
|---|---|---|---|
| $E_1$ | 1.50 | 0.045 | $2.2 \times 10^{-15}$ |
| $E_2$ | 1.50 | 0.140 | $1.2 \times 10^{-13}$ |
| $E_3$ | 0.40 | 0.300 | $6.2 \times 10^{-15}$ |
| $E_4$ | 0.08 | 0.760 | $3.1 \times 10^{-14}$ |
| $E_5$ | 0.10 | 0.960 | $1.9 \times 10^{-12}$ |
| Defects | $k$ (cm$^{-1}$) | $E_T$–$E_V$ (eV) | $\sigma_p$ (cm$^2$) |
| $H_0$ | 0.8 | 0.06 | $1.6 \times 10^{-16}$ |
| $H_1$ | 0.1–0.7 (assumed 0.4 in this work) | 0.29 | $5.0 \times 10^{-15}$ |
| $H_2$ | Not given (assumed 0.1 in this work) | 0.41 | $2.0 \times 10^{-16}$ |
| $H_3$ | 0.2 | 0.71 | $1.2 \times 10^{-14}$ |

only when both free electrons and holes have very large densities (heavily doped p–n junction or degenerated one) as is the case in a light emitting p–n diode or a laser p–n diode, which is not the case of the present study. We have also neglected possible communication between defect levels. This is due to the lack of work on GaAs on one hand and on the other hand it is observed that in amorphous silicon, for example, this phenomenon is only important at low temperatures [14]. This constitutes a good reason since usually amorphous silicon is more defected than GaAs, that is it has a much higher density of defects as well as them being more closely spaced in their distribution in the energy gap.

The solar cell used in this work has p$^+$ emitter and n$^+$ collector layers which are 0.02 and 0.04 $\mu$m thick, respectively, while the thickness of the n-type base region is 0.6 $\mu$m. The transparent layer used is glass/TCO (transparent conductive oxide). Its transmittance $T$ and the back reflection $R$ of the n/metal contact are taken into account. These are included in the generation rate $G$ distribution. When an AM0 solar spectrum (figure 1(a) [15]) is used to simulate space conditions (AM0 the sunlight outside the earth's atmosphere), $G$ is given by the following expression:

$$G(x) = \sum_\lambda T\alpha(\lambda)\phi(\lambda)[\exp(-\alpha(\lambda)x)$$
$$+ R\exp(-\alpha(\lambda)(2d - x))] \tag{6}$$

where $\alpha$ is the absorption coefficient, $\phi$ is the photon flux and $d$ is the thickness of the solar cell. Both $\alpha$ and $\phi$ depend on the wavelength $\lambda$. The absorption coefficient for GaAs is presented in figure 1(b) [16] and the photon flux is expressed as:

$$\phi(\lambda) = I(\lambda)\frac{\lambda}{hc} \tag{7}$$

where $I(\lambda)$ is the AM0 spectrum intensity and $hc/\lambda$ is the energy carried by a photon. The obtained generation rate profile will be presented later since it will be compared to the different defect level recombination rates (figure 3). The parameters used in the numerical simulation are listed in table 2.

simplified analytical model is a forced mathematical approach. The recombination centre parameters extracted in this way can be simply false. However, by using the full SRH formula (relation (5)) we show in the present study that the commonly used simplification is not justified since we found that the degradation cannot be restricted to one dominant defect (a recombination centre).

The introduction rate $k$ (the proportionality between the defect density and the irradiation fluence), the energy position and the capture cross section of each defect used in this work are summarized in table 1 [4, 5]. For the electron traps ($E_1$, $E_2$, $E_3$, $E_4$ and $E_5$) a high ratio of the capture cross sections for electrons with respect to that of holes is assumed, that is $\sigma_n/\sigma_p = 100$. Oppositely, $\sigma_p/\sigma_n = 100$ is assumed for the hole traps ($H_0$, $H_1$, $H_2$ and $H_3$). For the middle gap levels ($E_4$ and $H_3$) we have also added a particular case when they have a ratio $\sigma_n/\sigma_p \approx 1$ since they are considered as recombination centres [4]. In the initial state (before irradiation) we suppose that native defects have a very low density (about $10^{12}$ cm$^{-3}$) which is a typical requirement of good quality solar cells used for space applications. We also suppose that they can be grouped in a single recombination centre with capture cross sections of $\sigma_n = 10^{-13}$ cm$^{-2}$ and $\sigma_p = 10^{-15}$ cm$^{-2}$ [4, 5]. The different defect densities are obtained by the product $k \cdot \Phi$ where $\Phi$ (cm$^{-2}$) is the irradiation fluence.

In the present model we have neglected Auger and radiative recombination since they have a considerable effect
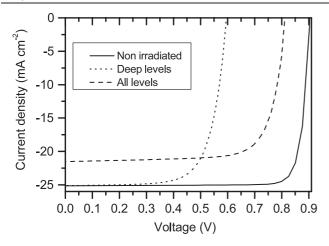
**Figure 2.** The numerically calculated $J$–$V$ characteristics before and after irradiation ($\sigma_n/\sigma_p = 100$).

**Table 2.** The solar cell parameters used in the simulation.

| Symbol | Parameter | Value |
|---|---|---|
| $E_g$ | Energy gap (eV) | 1.43 |
| $N_a$ | p$^+$-layer doping density (cm$^{-3}$) | $5 \times 10^{17}$ |
| $N_d$ | n-layer doping density (cm$^{-3}$) | $1 \times 10^{15}$ |
| $N_d$ | n$^+$-layer doping density (cm$^{-3}$) | $1 \times 10^{17}$ |
| $\Phi$ | Irradiation fluence (dose) (cm$^{-2}$) | $1 \times 10^{17}$ |
| $N_{nd}$ | Native defect density (cm$^{-3}$) (located at 0.7 eV) | $1 \times 10^{12}$ |
| $\sigma_{no}$ | Electron capture cross section for native defects | $1 \times 10^{-13}$ cm$^2$ |
| $\sigma_{po}$ | Hole capture cross section for native defects | $1 \times 10^{-15}$ cm$^2$ |
| $T$ | Glass/TCO transmittance | 0.8 |
| $R$ | n/metal contact reflectivity | 0.8 |

The effect of irradiation-induced defects is simulated by considering two cases. The first when only deep levels (E$_5$, E$_4$ and H$_3$) are introduced. The second when both deep (E$_5$, E$_4$ and H$_3$) and less deep levels (E$_1$, E$_2$, E$_3$, H$_0$, H$_1$ and H$_2$) are taken into account. The aim of this is to clearly distinguish the effect of each defect category on the output parameters of the cell.

## 3. Results and discussion

Figure 2 shows the calculated current–voltage characteristics ($J$–$V$) before irradiation and after irradiation in the two cases where only deep levels and all levels are taken into account. The extracted output parameters of the cell $J_{sc}$, $V_{oc}$, FF and $\eta$ before irradiation are 25.14 mA cm$^{-2}$, 0.90 V, 0.86, 19.60%, respectively. These parameters are in fairly good agreement with standard values of GaAs solar cells [17, 18]. They are also comparable to the $J$–$V$ curves obtained by SILVACO/Atlas [19]. From figure 2 it is clear that the short circuit current $J_{sc}$ is hardly affected by the presence of only deep levels while $V_{oc}$, FF and $\eta$ undergo a strong unreasonable reduction. This is in contrast with experimental observations where $J_{sc}$ exhibits a significant sensitivity to irradiation which is usually attributed to these deep levels or recombination



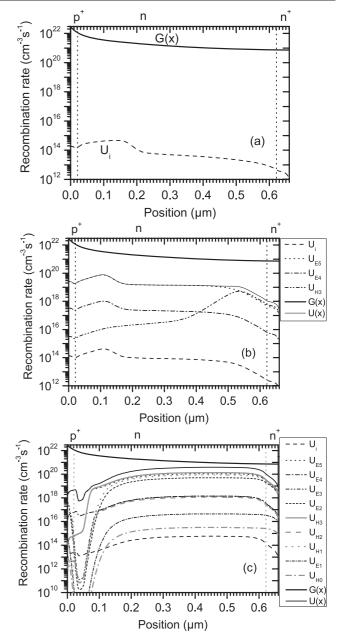**Figure 3.** Generation and recombination rates in the short circuit condition (a) before irradiation ($U_i$ is the intrinsic recombination rate related to native defects), (b) after irradiation taking into account only deep levels $\sigma_n/\sigma_p = 100$ and (c) after irradiation taking into account all levels $\sigma_n/\sigma_p = 100$ ($U(x)$ is the total recombination rate).

centres [4]. However, the addition of less deep levels engenders further sensitivity of $J_{sc}$ while the $V_{oc}$, FF and $\eta$ deteriorations are more reasonable. The extracted solar cell parameters from the $J$–$V$ characteristics of figure 2 are summarized in table 3.

As mentioned before, recombination centres can have a $\sigma_n/\sigma_p$ ratio close to unity which means an increase in the corresponding recombination rate by 100. In this case, we can see from table 3 that there is a slight reduction in the output parameters of the solar cell, for example $\eta$ is slightly reduced from 10.70% to 9.75% when only deep levels are present and from 13.27% to 12.74% in the presence of all levels.

To explain the $J_{sc}$ dependency on defect levels, we plotted in figure 3 the recombination rates corresponding to each
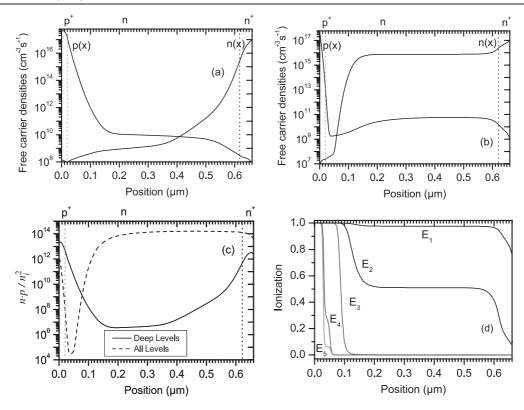
**Figure 4.** The *n* and *p* profile in the short circuit condition (a) after irradiation taking into account only deep levels, (b) after irradiation taking into account all levels, (c) $n \cdot p / n_i^2$ ratio for cases (a) and (b), and (d) the ionization of electron traps.

**Table 3.** The extracted output parameters of the solar cell before irradiation and after irradiation, when only deep levels are considered and when all levels are taken into account.

|  | $J_{sc}$ (mA cm$^{-2}$) | $V_{oc}$ (V) | FF | $\eta$ (%) |
|---|---|---|---|---|
| Before irradiation | 25.14 | 0.90 | 0.86 | 19.60 |
| Deep levels only | 25.11 | 0.56 | 0.71 | 10.70 |
| Deep levels only when $\sigma_n/\sigma_p = 1$ for $E_4$, $H_3$ | 25.03 | 0.56 | 0.69 | 09.75 |
| All levels | 21.51 | 0.81 | 0.76 | 13.27 |
| All levels, when $\sigma_n/\sigma_p = 1$ for $E_4$, $H_3$ | 21.13 | 0.80 | 0.75 | 12.74 |

of the previous cases compared to the photogeneration rate, in the short circuit condition. It is well known, according to free carrier continuity equations, that the current density is proportional to $\int (G(x) - U(x))dx$, where $U(x)$ is the recombination rate. Then any reduction of the difference $G(x) - U(x)$ will decrease the current density. In figure 2(a) (before irradiation) and (b) (when only deep levels are taken into account) the recombination rate is negligible with respect to the generation rate hence the current is solely due to photogeneration. In case (c), however, where all levels are taken into account there is an important reduction in $G(x) - U(x)$ since the recombination rate becomes comparable to the generation rate, hence the current density is greatly reduced. Moreover, in this case it is noticed that there is a significant increase in the deep level recombination rates compared to the case of their presence alone. Then the recombination centres' effect is effectively dominant but by taking into account all

defect levels. Therefore when characterizing irradiation related degradation, all created defects have to be taken into account and not only recombination centres as is usually done in some experimental work, see [4] for example.

To explain the recombination rate profile set by the different defect levels, we plot those of *n*, *p* and $n \cdot p / n_i^2$ in figures 4(a)–(c) where the two cases of deep levels only and all levels are taken into account; $n_i$ is the intrinsic density. These curves correspond also to the short circuit condition.

From figure 4(b), we notice that there is a considerable increase in *n* in the *n*-base region as all defect levels are introduced, while *p* decreases in the left side of the device. This is reproduced on the $n \cdot p$ profile that appears as the predominant term in the dominant recombination rate profile (figure 3(c)).

In figure 4(d) we plot the ionization of the electron traps to give an explanation of the low density of electrons in the n-doped base region when only deep levels are considered and the drastic change when all levels are introduced. The base region has a doping density of $10^{15}$ cm$^{-3}$ while the more deep electron traps $E_5$ and $E_4$ (with densities of $8 \times 10^{15}$ and $10^{16}$ cm$^{-3}$, respectively) are fully occupied which leads to an important decrease in the free electron density in this region. However, when other electron traps (less deep and shallow) are considered there is a considerable increase in the electron density owing to the ionization of these traps. The hole density in the n-type base side of the emitter–base interface is simply a spill-over of holes from the much higher doped p-type emitter.

## 4. Conclusion

The photo current voltage characteristics of a GaAs p$^+$–n–n$^+$ solar cell are numerically calculated before and after irradiation by energetic electrons. The changes induced by electron irradiation in the output parameters of a GaAs p$^+$–n–n$^+$ solar cell are extracted from these characteristics. The electron irradiation creates several defects which act as either recombination centres (deep levels) or traps (less deep levels). It was shown that the irradiation degradation cannot be only restricted to recombination centres or deep levels. The presence of less deep levels with the deep ones has a more pronounced and particular effect on the short circuit current in contrast to what is believed from some experimental work which cannot separate the different effects of the different types of defects. Taking into account less deep levels in addition to deep levels also provided reasonable degradation magnitudes for the other parameter in comparison with the case when only deep levels are taken into account. Therefore special care should be taken when relating the degradation of the solar cell to the defect due to irradiation by energetic particles such as electrons. In particular enormous errors can be made in evaluating defect parameters directly from the solar cell parameter degradation.

## Appendix. Numerical solution [11]

The device structure is divided into $N$ points along the $x$-axis. The values of $\psi(x)$, $n(x)$, $p(x)$ are defined at the principal points $x(h)$ while the derivatives to $x$ at the auxiliary points $z(\eta)$. The derivatives according to the finite difference method are given by:

$$\frac{dn}{dx}(\eta) = \frac{n(h) - n(h-1)}{\delta x(h)} \tag{A.1}$$

$$\frac{dp}{dx}(\eta) = \frac{p(h) - p(h-1)}{\delta x(h)} \tag{A.2}$$

$$\frac{d\psi}{dx}(\eta) = \frac{\psi(h) - \psi(h-1)}{\delta x(h)} \tag{A.3}$$

$$\frac{dJ_n}{dx}(h) = \frac{J_n(\eta+1) - J_n(\eta)}{\delta z(\eta)} \tag{A.4}$$

$$\frac{dJ_p}{dx}(h) = \frac{J_p(\eta+1) - J_p(\eta)}{\delta z(\eta)} \tag{A.5}$$

$$\xi(\eta) = -\frac{d\psi}{dx}(\eta) = \frac{\psi(h-1) - \psi(h)}{\delta x(h)} \tag{A.6}$$

$$\Delta\psi(h) = \frac{\xi(\eta) - \xi(\eta+1)}{\delta z(\eta)}. \tag{A.7}$$

Then the discretized form of the Poisson equation is:

$$F^\psi(h) = \gamma_1(h)\psi(h-1) + \gamma_2(h)\psi(h)$$
$$+ \gamma_3(h)\psi(h+1) + \frac{\rho(h)}{\varepsilon_r \varepsilon_o} = 0 \tag{A.8}$$

where $\gamma_1(h) = \dfrac{1}{\delta x(h)\delta z(\eta)}$,

$$\gamma_2(h) = -\frac{1}{\delta z(\eta)}\left(\frac{1}{\delta x(h)} + \frac{1}{\delta x(h+1)}\right),$$

$$\gamma_3(h) = \frac{1}{\delta x(h+1)\delta z(\eta)} \qquad \text{and} \tag{A.9}$$

$$\rho(h) = q\left(p(h) - n(h) + \sum_j p_t^j(h)\right.$$
$$\left. - \sum_j n_t^j(h) + N_{AD}(h)\right).$$

$\sum_j p_t^j(h)$ is the positive charge density of donor-like traps (electron traps), $\sum_j n_t^j(h)$ is the negative charge density of acceptor-like traps (hole traps), $N_{AD}(h)$ is the doping charge density.

The discretized forms of the continuity equations are:

$$F^n(h) = \frac{1}{\delta z(\eta)}\left(-\frac{\lambda_{n1}(\eta)}{\delta x(h)}n(h-1)\right.$$
$$+ \left(\frac{\lambda_{n1}(\eta+1)}{\delta x(h+1)} - \frac{\lambda_{n2}(\eta)}{\delta x(h)}\right)n(h)$$
$$\left. + \frac{\lambda_{n2}(\eta+1)}{\delta x(h+1)}n(h+1)\right) + G(h) - U_R(h) = 0 \tag{A.10}$$

$$F^p(h) = \frac{1}{\delta z(\eta)}\left(-\frac{\lambda_{p1}(\eta)}{\delta x(h)}p(h-1)\right.$$
$$+ \left(\frac{\lambda_{p1}(\eta+1)}{\delta x(h+1)} - \frac{\lambda_{p2}(\eta)}{\delta x(h)}\right)p(h)$$
$$\left. + \frac{\lambda_{p2}(\eta+1)}{\delta x(h+1)}p(h+1)\right) - G(h) + U_R(h) = 0. \tag{A.11}$$

By using the Gummel approximation we obtain for the current densities:

$$J_n(\eta+1) = \frac{q}{\delta x(h+1)}[\lambda_{n1}(\eta+1)n(h)$$
$$+ \lambda_{n2}(\eta+1)n(h+1)] \tag{A.12}$$

$$J_p(\eta+1) = \frac{q}{\delta x(h+1)}[\lambda_{p1}(\eta+1)p(h)$$
$$+ \lambda_{p2}(\eta+1)p(h+1)] \tag{A.13}$$

where

$$\beta(\eta+1) = \theta[\psi(h) - \psi(h+1)], \qquad \theta = \frac{q}{k_B T}$$

$$\lambda_{n1}(\eta+1) = \mu_n\left(\frac{\psi(h) - \psi(h+1)}{1 - \exp(\beta(\eta+1))}\right),$$

$$\lambda_{n2}(\eta+1) = \mu_n\left(\frac{\psi(h) - \psi(h+1)}{1 - \exp(-\beta(\eta+1))}\right)$$

$$\lambda_{p1}(\eta+1) = \mu_p\left(\frac{\psi(h) - \psi(h+1)}{1 - \exp(-\beta(\eta+1))}\right),$$

$$\lambda_{p2}(\eta+1) = \mu_p\left(\frac{\psi(h) - \psi(h+1)}{1 - \exp(\beta(\eta+1))}\right).$$

At the front contact we have:

$$F^{\mathrm{n}}(1) = \frac{1}{\delta z(1)}\left(-S_{\mathrm{n}}(n(1)-n_{\mathrm{eq}}) + \frac{\lambda_{\mathrm{n1}}(2)}{\delta x(2)}n(1)\right.$$
$$\left. + \frac{\lambda_{\mathrm{n2}}(2)}{\delta x(2)}n(2)\right) + G(1) - U(1) = 0 \qquad (A.14)$$

$$F^{\mathrm{p}}(1) = \frac{1}{\delta z(1)}\left(-S_{\mathrm{p}}(p(1)-p_{\mathrm{eq}}) + \frac{\lambda_{\mathrm{p1}}(2)}{\delta x(2)}p(1)\right.$$
$$\left. + \frac{\lambda_{\mathrm{p2}}(2)}{\delta x(2)}p(2)\right) - G(1) + U(1) = 0 \qquad (A.15)$$

while at the back contact we have:

$$F^{\mathrm{n}}(N) = \frac{1}{\delta z(N)}\left(-\frac{\lambda_{\mathrm{n1}}(N)}{\delta x(N)}n(N-1) - \frac{\lambda_{\mathrm{n2}}(N)}{\delta x(N)}n(N)\right.$$
$$\left. + S_{\mathrm{n}}(n(N)-n_{\mathrm{eq}})\right) + G(N) - U(N) = 0 \qquad (A.16)$$

$$F^{\mathrm{p}}(N) = \frac{1}{\delta z(N)}\left(-\frac{\lambda_{\mathrm{p1}}(N)}{\delta x(N)}p(N-1) - \frac{\lambda_{\mathrm{p2}}(N)}{\delta x(N)}p(N)\right.$$
$$\left. + S_{\mathrm{p}}(p(N)-n_{\mathrm{eq}})\right) - G(N) + U(N) = 0. \qquad (A.17)$$

Then the complete set of discretized equations has the following form:

$$\begin{pmatrix} F(1) \\ F(2) \\ \vdots \\ F(h) \\ \vdots \\ F(N) \end{pmatrix} = 0, \qquad \text{where } F(h) = \begin{pmatrix} F^{\psi}(h) \\ F^{\mathrm{n}}(h) \\ F^{\mathrm{p}}(h) \end{pmatrix}. \quad (A.18)$$

We have used the Newton iterative method which uses:

$$y^{s+1} = y^s - \frac{F(y^s)}{F'(y^s)} \ (s \text{ is the iteration step}) \qquad (A.19)$$

to solve (A.18) by transforming it to the form:

$$\underbrace{\begin{pmatrix} B(1), C(1), 0, \ldots\ldots\ldots, 0 \\ A(2), B(2), C(2), 0, \ldots\ldots 0 \\ 0, A(3), B(3), C(3), 0, \ldots, 0 \\ \vdots \\ 0, \ldots 0, A(h), B(h), C(h), \ldots, 0 \\ \vdots \\ 0, \ldots\ldots 0, A(N), B(N) \end{pmatrix}}_{M_t}$$

$$\underbrace{\begin{pmatrix} \delta y(1) \\ \delta y(2) \\ \vdots \\ \delta y(h) \\ \vdots \\ \delta y(N) \end{pmatrix}}_{\delta y} = -\underbrace{\begin{pmatrix} F(1) \\ F(2) \\ \vdots \\ F(h) \\ \vdots \\ F(N) \end{pmatrix}}_{F} \qquad (A.20)$$

where

$$A(h)\delta y(h-1) + B(h)\delta y(h) + C(h)\delta y(h+1) = -F(h)$$

and

$$\delta y(h) = \begin{pmatrix} \delta \psi(h) \\ \delta n(h) \\ \delta p(h) \end{pmatrix}.$$

## References

[1] Yamaguchi M 2001 Radiation-resistant solar cells for space use *Sol. Energy Mater. Sol. Cells* **68** 31–53
[2] Bourgoin J C and de Angelis N 2001 Radiation-induced defects in solar cell materials *Sol. Energy Mater. Sol. Cells* **66** 467–77
[3] de Angelis N, Bourgoin J C, Takamoto T, Khan A and Yamaguchi M 2001 Solar cell degradation by electron irradiation. Comparison between Si, GaAs and GaInP cells *Sol. Energy Mater. Sol. Cells* **66** 495–500
[4] Bourgoin J C and Zazoui M 2002 Irradiation-induced degradation in solar cell: characterisation of recombination centres *Semicond. Sci. Technol.* **17** 453–60
[5] Pons D and Bourgoin J C 1985 Irradiation-induced defects in GaAs *J. Phys. C: Solid State Phys.* **18** 3839–71
[6] Mbarki M, Sun G C and Bourgoin J C 2004 Prediction of solar cell degradation in space from the electron–proton equivalence *Semicond. Sci. Technol.* **19** 1081–5
[7] Hadrami M, Roubi L, Zazoui M and Bourgoin J C 2006 Relation between solar cell parameters and space degradation *Sol. Energy Mater. Sol. Cells* **90** 1486–97
[8] Warner J H, Messenger S R, Walters R J, Summers G P, Lorentzen J R, Wilt D M and Smith M A 2006 Correlation of electron radiation induced-damage in GaAs solar cells *IEEE Trans. Nucl. Sci.* **53** 1988–94
[9] Schockley W and Read W T 1952 Statistics of the recombination of holes and electrons *Phys. Rev.* **87** 835
[10] Hall R N 1952 Eletron–hole recobination in germanium *Phys. Rev.* **87** 387
[11] Kurata M 1982 *Numerical Analysis for Semiconductor Devices* (Lexington, MA: Heath)
[12] Sze S M 1982 *Physics of Semiconductor Devices* 2nd edn (New York: Wiley)
[13] Zazoui M, Bourgoin J C, Stievenard D, Deresmes D and Strobl G 1994 Recombination centers in electron-irradiated Czochralski silicon solar cells *J. Appl. Phys.* **76** 15
[14] Zeman M, van den Heuvel J, Kroon M and Willemen J 2000 Amorphous semiconductor analysis (ASA) *USER'S MANUAL Version* 3.3 Delft Univ. of Technology, Delft, the Netherlands
[15] Equer B 1993 Energie solaire photovoltaique, Tome 1: Physique et technologie de la conversion photovoltaique *Ellipses* UNESCO, Paris
[16] Mathieu H 1996 *Physique Des Semiconducteurs et Des Composants Électroniques* 3rd edn (Paris: Masson)
[17] Green M A, Emery K, King D L, Igari S and Warta W 2003 Solar cell efficiency tables (Version 21) *Prog. Photovolt: Res. Appl.* **11** 39–45
[18] Chandrasekaran N, Soga T, Inuzuka Y, Imaizumi 1 M, Taguchi H and Jimbo T 2005 1 MeV electron irradiation effects of GaAs/Si solar cells *Mater. Res. Soc. Symp. Proc.* **836** L6.7.1–6
[19] Michael S 2005 A novel approach for the modelling of advanced photovoltaic devices using the SILVACO/ATLAS virtual wafer fabrication tools *Sol. Energy Mater. Sol. Cells* **87** 771–84